ELSEVIER

European Journal of Cancer 40 (2004) 1441–1452

European Journal of Cancer

www.ejconline.com

Sodium butyrate induces apoptosis in human hepatoma cells by a mitochondria/caspase pathway, associated with degradation of β-catenin, pRb and Bcl-X_L

S. Emanuele, A. D'Anneo, G. Bellavia, B. Vassallo, M. Lauricella, A. De Blasio, R. Vento, G. Tesoriere *

Dipartimento di Biologia Cellulare e dello Sviluppo, Sezione di Biochimica, Università di Palermo, Policlinico, Via del Vespro 129, 90127 Palermo, Italy

Received 21 January 2004; accepted 26 January 2004
Available online 9 April 2004

Abstract

Butyrate can promote programmed cell death in a number of tumour cells in vitro. This paper provides evidence that butyrate induces apoptosis in human hepatoma HuH-6 and HepG2 cells but is ineffective in Chang liver cells, an immortalised non-tumour cell line. In both HuH-6 and HepG2 cells, apoptosis appeared after a lag period of approximately 16 h and increased rapidly during the second day of treatment. In particular, the effect was stronger in HuH-6 cells, which were, therefore, chosen for ascertaining the mechanism of butyrate action. In HuH-6 cells, β-catenin seemed to exert an important protective role against apoptosis, since pretreatment with β-catenin antisense ODN reduced the content of β-catenin and anticipated the onset of apoptosis at 8 h of exposure to butyrate. Moreover, in HuH-6 cells, butyrate induced loss of mitochondrial membrane potential, release of cytochrome *c* from mitochondria, activation of caspase 9 and caspase 3, and degradation of poly(ADP-ribose) polymerase. In addition, during the second day of treatment, β-catenin, pRb, and cyclins D and E were diminished and the phosphorylated form of pRb disappeared. Also, the content of the anti-apoptotic factor Bcl-X_L fell markedly during this period, while that of the pro-apoptotic factor Bcl-Xs increased. These effects were accompanied by an increase in both Bcl-X_L and Bcl-Xs mRNA transcripts, as ascertained by reverse transcriptase-polymerase chain reaction. Our results suggest that caspases have a crucial role in butyrate-induced apoptosis. This conclusion is supported by the observation that the inhibitors of caspases, benzyloxy carbonyl-Val-Ala-Asp-fluoromethylketone and benzyloxy carbonyl-Asp-Glu-Val-Asp-fluoromethylketone, prevented apoptosis and the decrease in Bcl-X_L, pRb, cyclins and β-catenin. These effects were most probably responsible for the increased sensitivity of the cells to butyrate-induced apoptosis, which was observed on the second day of treatment.

Keywords: β-Catenin; pRb; Apoptosis

1. Introduction

Butyrate is a short-chain fatty acid, naturally present in the human colon as a micronutrient produced by the bacterial fermentation of fibres, that can inhibit cell growth and promote differentiation in normal and tumour cell lines [1]. To explain these effects, evidence has been provided that butyrate acts as an inhibitor of histone deacetylase, thereby inducing histone hyperacetylation, chromatin relaxation and changes in the expression of some regulatory genes [2]. In particular, it has been documented that butyrate can induce cell-cycle arrest by increasing the expression of p21/WAF-1 and p27/KIP-1 [3,4], and differentiation by upregulating a number of biochemical markers, such as cytokeratin 19 [5], alkaline phosphatase [6], integrin-β_1 and osteopontin [7].

Apart from effects on the cell cycle and differentiation, butyrate can also stimulate apoptosis in many cancer cells [8–11], including breast and colon cancer, glioma and mesothelioma cell lines, by inducing a p53-independent pathway, which can be correlated with the activation of the Fas/FasL system [12] or with changes in the contents of proteins of the Bcl-2 family

* Corresponding author. Tel.: +39-91-6552459; fax: +39-91-6552449.
E-mail address: gtesor@unipa.it (G. Tesoriere).

0959-8049/$ - see front matter © 2004 Elsevier Ltd. All rights reserved.
doi:10.1016/j.ejca.2004.01.039

[13]. An apoptotic effect of butyrate has been also demonstrated in several human hepatoma cell lines and has been correlated with increased expression of p21WAF1 or p27Kip1 [14–16].

In our previous paper we showed that, in human retinoblastoma Y79 cells, butyrate was able to exert a clear apoptotic effect by reducing the amount of Bcl-2 and inducing the activity of 26S proteasome, with a consequent decrease in the content of p53 and other short-lived proteins [17]. We also showed that the effect was increased synergistically when butyrate was associated with the inhibitor of topoisomerase I, camptothecin [18], or the proteasome inhibitor MG132 [17].

We have recently focused our interest on liver cancer. The global incidence of this tumour has increased considerably in recent years and it has become one of the most frequent malignant neoplasms. Viral B and C infections are considered the principal causal agents [19,20], while exposure to specific compounds, such as aflatoxin B_1 [20] or diethylnitrosamine [21], may contribute to hepatocarcinogenesis. However, the molecular mechanisms leading to liver tumour transformation and progression are still unclear. Recent studies have demonstrated that alterations in the β-catenin gene are frequent in human hepatocellular carcinomas. The aberrant accumulation of β-catenin, due to genetic mutations affecting either β-catenin itself or its regulatory factors, such as APC or axin, has been shown to play an important oncogenic role in various tumour types, including colorectal and hepatic cancers [22,23].

In this study we investigated the molecular mechanism by which butyrate induces apoptosis in human hepatoma HuH-6 and HepG2 cells, two cell lines characterised by the accumulation of β-catenin. We show that butyrate induces apoptosis in both cell lines through a mitochondria caspase-dependent pathway. The activation of caspases caused a fall in the contents of β-catenin, pRb, cyclins and Bcl-X_L. A possible relation between this decrease and an increase in the sensitivity of hepatoma cells to butyrate-induced apoptosis is discussed.

2. Materials and methods

2.1. Cell cultures and reagents

HuH-6, HepG2 and Chang liver cell lines were kindly provided by Dr. M. Cervello (Centro Nazionale Ricerche, Palermo). Cells were grown as monolayers in RPMI 1640 medium, supplemented with 10% (v/v) heat-inactivated fetal calf serum (FCS) and 1.0 mM sodium pyruvate, in a humidified atmosphere containing 5% CO_2, at 37 °C. Unless stated otherwise, incubations were performed with HuH-6 cells and HepG2 cells seeded on 96-well plates or 100-mm culture dishes. After plating, cells were allowed to adhere overnight and were then treated with chemical or vehicle only (control samples). Cell viability was determined, as previously reported [24], by the MTT quantitative colorimetric assay, capable of detecting viable cells.

Sodium butyrate was obtained from Sigma (St. Louis, MO). Benzyloxy carbonyl-Val-Ala-Asp-fluoromethylketone (z-VAD-fmk) was supplied by Promega (Italy) and benzyloxy carbonyl-Asp-Glu-Val-Asp-fluoromethylketone (z-DEVD-fmk) by Calbiochem (Germany).

2.2. Assessment of apoptosis and cell-cycle analysis

Apoptotic morphology was studied as previously reported [24] by staining the cells with a combination of the fluorescent DNA-binding dyes acridine orange and ethidium bromide, 100 μg/ml phosphate-buffered saline (PBS) for each dye. The differential uptake of these two dyes allowed the identification of viable and non-viable cells by fluorescence microscopy. Normal nuclei in live cells appeared bright green; apoptotic nuclei in dead cells appeared bright orange with highly condensed chromatin.

For cell-cycle analysis by flow cytometry, hepatoma cells (10^6 per condition) were harvested, washed and fixed with 70% ice-cold ethanol. The cells were resuspended in a hypotonic fluorochrome solution (50 μg/ml propidium iodide, 0.1% sodium citrate, 0.1% Nonidet P-40 and 100 μg/ml RNase A) and incubated in the dark at 4 °C overnight. Propidium iodide (PI) staining of DNA from 10.000 cells was detected on FACScan flow cytometer (Beckman Coulter Epics XL) and the proportion of cells giving fluorescence in the hypodiploid sub-G0/G1 peak of the cell cycle was taken as a measure of apoptosis. All data were recorded and analysed using *Expo32* software.

2.3. Measurement of mitochondrial transmembrane potential ($\Delta\psi_m$)

Cells were harvested and incubated with 40 nM 3,3-dihexyloxacarbocyanine ($DiOC_6$; Molecular Probes, Eugene, OR) for 20 min at 37 °C, washed twice with PBS, and analysed by flow cytometry on an EPICS XL (Coulter Electronics) FACScan. Excitation was at 488 and 525 nm with a dichroic LP filter.

The percentage of cells showing less fluorescence, reflecting loss of mitochondrial transmembrane potential, was determined by comparison with untreated controls using *Expo32* software. Carbonylcyanide *m*-chlorophenylhydrozone (CCCP; 50 μM), a protonophore that completely de-energises mitochondria by dissipating the transmembrane potential, was used as a positive control.

2.4. Antisense inhibition of β-catenin expression

The specific phosphorothioate-modified β-catenin antisense oligonucleotide used in this study was 5′-ACT CAG CTT GGT TAG TGT GTC AGG C-3′. The oligonucleotide with the sequence 5′-CGG ACT GTG TGA TTG GTT CGA CTC A-3′ was employed as reverse-sequence control. The oligonucleotides were added to OPTIMEM medium in the presence of lipofectin (Life Technologies, Inc.), using 2 μl of lipofectin/ml of OPTIMEM medium/100 nM oligonucleotide. The preparation was then added to 70% confluent cells in 6-well plates. After 5 h, the transfection medium was replaced with RPMI containing 10% FCS and butyrate was added for various times.

2.5. Preparation of cytosolic and mitochondrial extracts

HuH-6 and HepG2 hepatoma cells (5×10^6) were washed twice with PBS and harvested by centrifugation (500*g* for 5 min). Cell pellets were resuspended in 350 μl of buffer A (20 mM Hepes, 1.5 mM $MgCl_2$, 10.0 mM KCl, 1.0 mM EDTA, 1.0 mM EGTA, 1.0 mM dithiothreitol and 250 mM sucrose) containing protease inhibitors (0.1 mM phenylmethylsulphonyl fluoride and 10.0 μg/ml leupeptin, aprotinin and pepstatin A). Cells were homogenised on ice in Dounce homogeniser (30 strokes) and centrifuged at 2000*g* for 10 min at 4 °C. Supernatant (S1) was collected and the pellet again homogenised in buffer A to obtain a new supernatant (S2). S1 and S2 were mixed and centrifuged at 11,000*g* for 10 min. The pellet and the supernatant represent mitochondrial and cytosolic fractions, respectively.

2.6. Western blotting

Cell lysates were prepared as described previously [24]. Protein concentration was determined by Lowry assay. Equal amounts (50 μg/lane) of protein samples were resolved by sodium dodecyl sulphate–polyacrylamide gel electrophoresis and electroblotted on to nitrocellulose for detection with primary antibodies followed by specific secondary antibodies conjugated with alkaline phosphatase. The loading homogeneity was checked by staining the membrane with red S Ponceau. Visualisation was performed using nitroblue tetrazolium and bromo-chloro-indoyl-phosphate. For detection of β-catenin protein, horseradish peroxidase-conjugated secondary antibody (Amersham) was employed, followed by visualisation with an enhanced chemiluminescence system (Amersham). Bands were quantified by densitometric analysis using SMX *Image* software. All antibodies employed were purchased from Santa Cruz Biotechnology (Santa Cruz, CA, USA). Both Bcl-X isoforms were evidenced by using Bcl-$X_{S/L}$ (L-19) rabbit polyclonal antibody. To detect both phospho-pRb and unphospho-pRb, IF-8 mouse monoclonal antibody, which recognises the A/B pocket, was used. Phospho-pRb was specifically evidenced by using the Phospho-Plus RB (Ser 780, Ser 795 and Ser 807/811) antibody kit obtained from Cell Signaling (Beverly, MA).

2.7. RNA extraction and reverse transcriptase-polymerase chain reaction

Total RNA was extracted from cells by a guanidinium isothiocyanate method according to Chomczynski and Sacchi [25]. Total RNA (1 μg) was reverse-transcribed using the GeneAmp Kit for reverse transcriptase-polymerase chain reaction (RT-PCR) (Perkin–Elmer).

To amplify the human *Bcl-X* gene, cDNA was subjected to PCR using the following oligonucleotide primers: 5′-TTGGACAATGGACTGGTTGA-3′ as the forward primer and 5′-GTAGAGTGGATGGTCAGTG-3′ as the reverse primer. As an internal control, human glyceraldehyde-3-phosphate dehydrogenase (G3PDH) cDNA was amplified using the forward primer 5′-TGACATCAAGAAGGTGGTGA-3′ and the reverse primer: 5′-TCCACCACCCTGTTGCTGTA-3′.

Following an initial denaturation step (94 °C for 1 min), amplifications were performed under the following reaction conditions: 94 °C for 1 min; 56 °C for 2 min; 72 °C for 3 min (20–25 cycles). The PCR was completed by a 10-min elongation step at 72 °C. The amplified products were resolved by agarose gel electrophoresis (1% agarose and 0.5 μg/ml ethidium bromide), and then photographed and scanned into Adobe *Photoshop*. Densitometric analysis of the bands was carried out as described in the previous section.

3. Results

3.1. Sodium butyrate-induced apoptosis in HuH-6 and HepG2 cells

The aim was to study the effects exerted by butyrate on monolayer cultures of HuH-6 and HepG2 human hepatoma cells, in comparison with Chang liver cells, an immortalised non-tumour cell line. HepG2 (10^4/well), HuH-6 (5×10^3/well) and Chang liver cells (5×10^3/well) were seeded in 96-well plates and maintained in culture for 24 h. Thereafter, butyrate was added at different concentrations and the incubation protracted for various times.

HuH-6 and HepG2 cells treated for short periods of time (8–16 h) with 2 mM butyrate appeared flattened, separated from each other and with dendrite-like cytoplasmic protrusions (Fig. 1(b)). When the incubation was for longer (24–48 h), a large proportion of cells

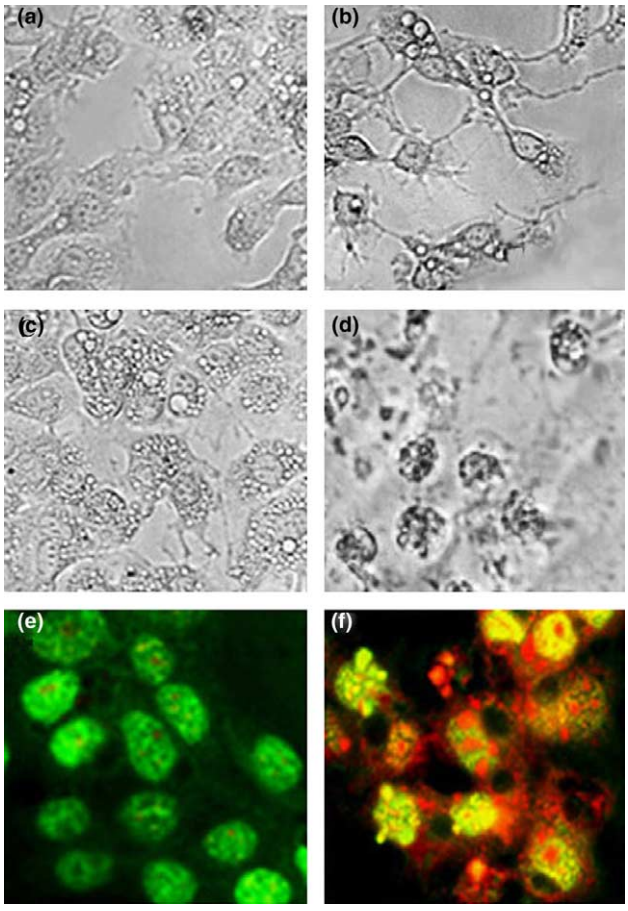

Fig. 1. Morphological effects induced by butyrate in HuH-6 cells. (a–d) Morphological analysis by conventional light microscopy. (e–f) Staining with acridine orange/ethidium bromide and analysis under fluorescence microscopy. HuH-6 cells cultured for 16 (a,b) or 48 h (c–f) without (a, c and e) or with 2 mM sodium butyrate (b, d and f). The figure is representative of three independent experiments. Four different visual fields examined for each condition. Photographs taken at a magnification of 400×.

showed the typical morphological features of apoptosis: a reduction in cell volume, chromatin condensation and nuclear fragmentation (Fig. 1(d)). In contrast, treatment with 2 mM butyrate for 8–48 h did not produce visible apoptotic effects in Chang liver cells (not shown).

In both hepatoma cell lines, butyrate-induced cell death was confirmed as apoptosis by the following: (i) fluorescence microscopy by dual staining with acridine orange/ethidium bromide showed that after treatment with butyrate most of the cells appeared orange-stained with highly condensed and fragmented chromatin (Fig. 1(f)); (ii) flow cytometric profiles of cell-cycle distribution showed that butyrate caused a remarkable increase in the percentage of cells included in the sub-G1 peak, representing cells with fragmented DNA (Fig. 2(a)); (iii) flow cytometric analysis also showed that the action of butyrate was completely suppressed by 100 μM z-VAD-fmk, a general inhibitor of caspases, and markedly reduced by 100 μM z-DEVD-fmk, a selective inhibitor of effector caspases (Fig. 2(a)). This last finding demonstrated that the activation of caspases, the proteolytic activity associated with apoptosis, was required for the induction of cell death by butyrate.

In flow cytometric analysis we calculated an apoptotic index as the percentage of cells found in the subdiploid region after PI staining. With 2 mM butyrate, apoptosis appeared at 24 h of treatment (Fig. 2(b)). The effect then increased with time so that after 48 h of exposure the proportion of dead cells reached 80.5% and 42% for HuH-6 and HepG2 cells, respectively. In contrast, butyrate produced only a marginal effect in Chang liver cells (Fig. 2(b)). The butyrate effect was also dose-dependent, the highest efficacy being observed with 2–5 mM butyrate (not shown). Because of the high sensitivity of HuH-6 cells to butyrate, this cell line was chosen to clarify the mechanism of the butyrate effect.

3.2. The effect of butyrate on β-catenin

Both HuH-6 and HepG2 cells have been found to contain high concentrations of altered forms of β-catenin [26]. In HuH-6 cells the β-catenin gene exhibits a point mutation. Thus, a mutated form of the protein with a normal molecular weight (92 kDa) accumulates in these cells. In HepG2 cells, the β-catenin gene exhibits a deletion of exons 3–4 and expresses a large amount of a truncated form of β-catenin (73 kDa), together with a smaller amount of the wild-type form.

Western blotting analysis (Fig. 3(a)), performed here with a monoclonal antibody that recognises an epitope located in the carboxyterminal region of β-catenin, confirmed these findings and in addition showed that Chang liver cells contain a low concentration of β-catenin. Treatment with 2 mM butyrate produced different effects on β-catenin in the three cell lines: in HuH-6 cells it caused a remarkable decrease in the 92-kDa band with the appearance of degradation forms of the protein; in HepG2 cells it induced a modest decrease in the wild-type form; in Chang liver cells the treatment did not affect the amount of β-catenin. The effect induced by butyrate in HuH-6 cells was dependent on the dose employed (Fig. 3(b)) and the length of treatment (Fig. 3(c)). In cells treated with 2 mM butyrate the decrease in β-catenin was modest in the first 16 h of treatment; the amount then fell to 45% of control after 24 h and to 20% after 48 h of exposure.

It has been previously reported [27] that β-catenin can be cleaved, with the production of 65–72 kDa fragments, in a caspase-dependent process that is associated with apoptosis. We confirm that the cleavage of β-catenin is determined by caspases, since in HuH-6 cells the decrease in β-catenin together with the production of degradation products were abolished by the addition of

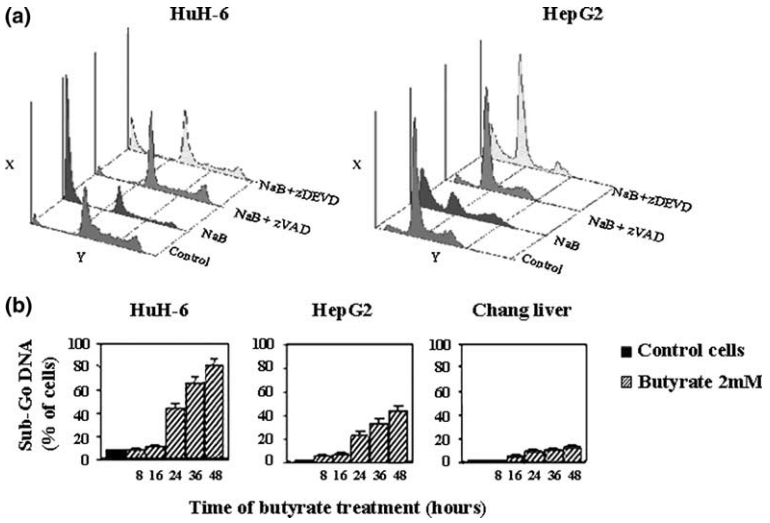

Fig. 2. The effect of butyrate on the cell-cycle distribution of HuH-6 and HepG2 cells. (a) Flow cytometric analysis of propidium iodide-stained HuH-6 cells or HepG2 cells treated with 2 mM sodium butyrate for 48 h without or with 100 μM z-VAD-fmk or 100 μM z-DEVD-fmk. The *x*-axis indicates fluorescence intensity on logarithmic scale. The *y*-axis indicates the number of events. (b) Apoptotic effects induced by increasing concentrations of butyrate in HuH-6, HepG2 and Chang liver cells. Percentages of cells in the sub-diploid region, evaluated by flow cytometry of propidium iodide-stained cells, comprise an index of apoptosis. The results represent means ± SEM of four independent experiments.

100 μM z-VAD-fmk and partially reduced by 100 μM z-DEVD-fmk (Fig. 3(b)).

In order to investigate whether β-catenin can exert an anti-apoptotic role, we pretreated HuH-6 cells for 5 h with β-catenin antisense ODN to reduce the concentration of the protein. Then ODN was removed and the samples were incubated without or with 2 mM butyrate for various times. Comparison between Fig. 3(c) and (d) demonstrates that pretreatment with β-catenin antisense ODN clearly reduced the amount of the protein. This effect was already visible at 8 h of incubation. Moreover, the anticipated effect of butyrate on the β-catenin was clearly observed also after brief periods of incubation (8–16 h) (Fig. 3(d)). In contrast, pretreatment of HuH-6 cells with reverse control ODN produced no change in the amount of β-catenin (not shown).

The results shown in Fig. 4(b) demonstrate that in ODN-treated cells apoptosis had appeared by 8 h of incubation, with approximately 15% of dead cells. This proportion increased to 30% after 16 h of treatment, while only a negligible number of apoptotic cells were observed in cells pretreated with reverse control ODN at both 8 and 16 h of treatment with butyrate (Fig. 4(a)). The addition of β-catenin antisense ODN also potentiated the apoptotic effect induced by butyrate at 24 h (65% of dead cells vs. 42% in control) and 48 h (85% vs. 80.5%) of treatment.

3.3. Butyrate caused dephosphorylation of pRb

It is well known that pRb, the product of the retinoblastoma gene, is a key regulator of the cell cycle and modulates cell proliferation and differentiation [28]. In particular, it has been shown that loss of pRb or the presence of the phosphorylated and inactive form of the protein can favour tumourigenesis [29]. Moreover, recent studies indicate that pRb serves a protective function against apoptosis in some cell systems [30,31]. In this regard it has been shown that pRb is first dephosphorylated and then proteolytically cleaved by caspases into p48 and p68 inactive fragments [32], and it has been suggested that the cleavage of pRb represents a permissive step in the apoptosis-inducing pathway [32,33].

In order to study the effect of butyrate on the amount of pRb and its phosphorylation state, we performed Western blotting analysis using, first, an antibody against the A/B pocket domain. Our results (Fig. 5(a)) demonstrated the presence of two distinct species, a slow-migrating form, corresponding to phosphorylated pRb (p110), and a fast-migrating form, which was related to unphosphorylated pRb (p105). When HuH-6 cells were treated with 2 mM butyrate, a decrease in the intensity of the band corresponding to phospho-pRb was observed by 16 h, while a decrease in the intensity of unphospho-pRb appeared at 24 h of exposure. During the second day of treatment the intensity of both bands further decreased, so that after 48 h the phospho-pRb had disappeared while the unphospho-pRb had fallen to about 30% of control and a cleavage product of about 100 kDa was visible (Fig. 5(a)). The effect on the phosphorylation state was confirmed using three antibodies that specifically recognise phosphoserines 807–811, phosphoserine 795 and phosphoserine 780, respectively (Fig. 5(b)).

Interestingly, the addition of z-VAD-fmk suppressed, during the course of the treatment (16–48 h), the

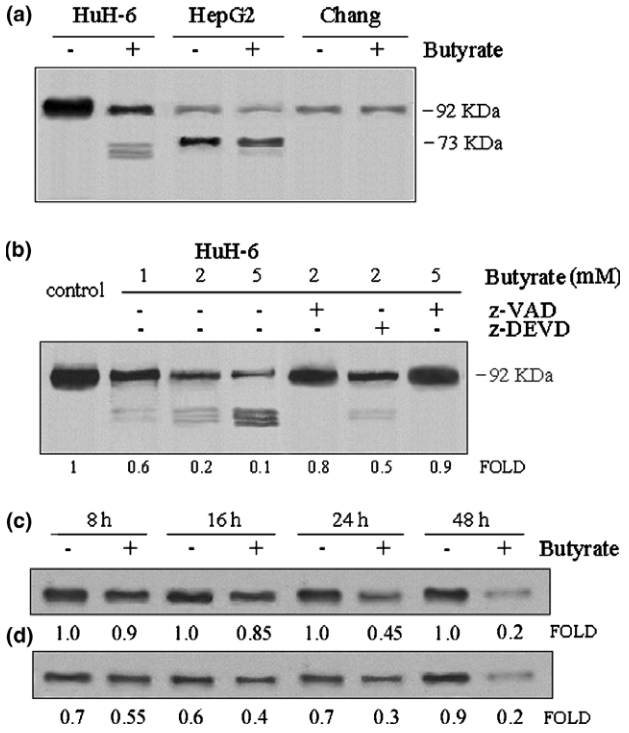

Fig. 3. The effect of butyrate on β-catenin. HuH-6, HepG2 and Chang liver cells treated for various times with sodium butyrate. Cell lysates prepared and analysed by Western blotting on duplicate samples. (a) Comparison between the effects exerted by 2 mM sodium butyrate for 48 h on β-catenin in HuH-6, HepG2 and Chang liver cells. (b) The effect of increasing concentrations of butyrate on β-catenin in HuH-6 cells and the influence of z-VAD-fmk and z-DEVD-fmk on this effect. (c,d) Time course of the effect induced by 2 mM sodium butyrate on β-catenin in HuH-6 cells untreated (c) or treated (d) with β-catenin antisense ODN. HuH-6 cells transfected for 5 h with β-catenin antisense ODN and then treated with 2 mM sodium butyrate for various times. Detection with an enhanced chemiluminescence system in order to visualise degradation products of β-catenin. The experiments were performed three times with similar results.

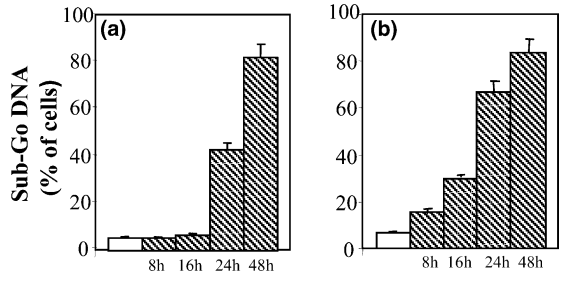

Fig. 4. The influence of β-catenin antisense ODN transfection on the apoptotic effect of butyrate in HuH-6 cells. HuH-6 cells transfected for 5 h with β-catenin antisense ODN (b) or reverse control ODN (a). Cells then treated with 2 mM butyrate for various times. Percentages of cells in sub-diploid region comprise an index of apoptosis. The results represent means ± SEM of four independent experiments.

depressant effect of butyrate on the unphosphorylated form of pRb and reduced that on the phosphorylated form (Fig. 5(a) and (b)). z-DEVD-fmk exerted a similar action, but with less efficacy (not shown).

Treatment of HepG2 cells with 2 mM butyrate also decreased the concentrations of the two forms of pRb, but the effect was modest compared to that found in HuH-6 cells. Finally, in Chang liver cells, butyrate induced a modest decrease only in phospho-pRb (Fig. 5(a)).

3.4. The effect of butyrate on the cyclins, CDKs, p21, p27 and p53

Phosphorylation of pRb occurs in the G1 phase of cell cycle by activation of cyclin-dependent kinases (CDKs), which are serine/threonine kinases dependent on the presence of G1-phase cyclins (cyclins D and E). The activity of cyclin-CDK complexes is inhibited by factors belonging to the Cip/kip family, such as p21 and p27. As shown in Fig. 6, treatment of HuH-6 cells with 2 mM butyrate markedly reduced the amount of both cyclins D and E. This effect was suppressed by z-VAD-fmk and reduced by z-DEVD-fmk. However, treatment of HuH-6 cells with butyrate did not modify the amounts of CDK2 and CDK4 or those of p21 and p27 (not shown).

In spite of the fundamental role exerted by the product of the tumour-suppressor gene p53 in many apoptotic pathways, butyrate-induced apoptosis is shown to be independent of p53 in many systems [12]. Our results demonstrate that treatment with butyrate caused a modest decrease in p53 in both HuH-6 and HepG2 cells (not shown). Thus, in hepatoma cells also the butyrate effect seemed to be independent of p53.

3.5. Effects of sodium butyrate on the expression of Bcl-2 family of proteins

The members of the Bcl-2 family of proteins are important regulators of apoptosis. In order to individuate the role exerted by these factors in butyrate-induced apoptosis, we first ascertained the presence of anti-apoptotic factors of this family in the cell lines used in our experiments. We observed that the anti-apoptotic factor Bcl-2 was undetectable in HuH-6 cells, while a low content was found in HepG2 cells. In contrast, non-tumour Chang liver cells exhibited a high content of this factor (not shown). We also analysed two products of the *Bcl-X* gene, Bcl-X_L, a Bcl-2 homologue with anti-apoptotic action, and Bcl-Xs, an alternatively spliced variant of the *Bcl-X* gene with pro-apoptotic activity. In extracts of the three cell lines a band of 31 kDa corresponding to Bcl-X_L was clearly identified, while Bcl-Xs was undetectable. Treatment of HuH-6 cells with 2 mM butyrate for 24 h (Fig. 7(a)) induced a decrease in Bcl-X_L and the appearance of a 21-kDa band corresponding to Bcl-Xs. After 48 h, the effects were more evident, with a remarkable increase in the intensity of the 21-kDa band, whereas the amount of Bcl-X_L decreased to 30%

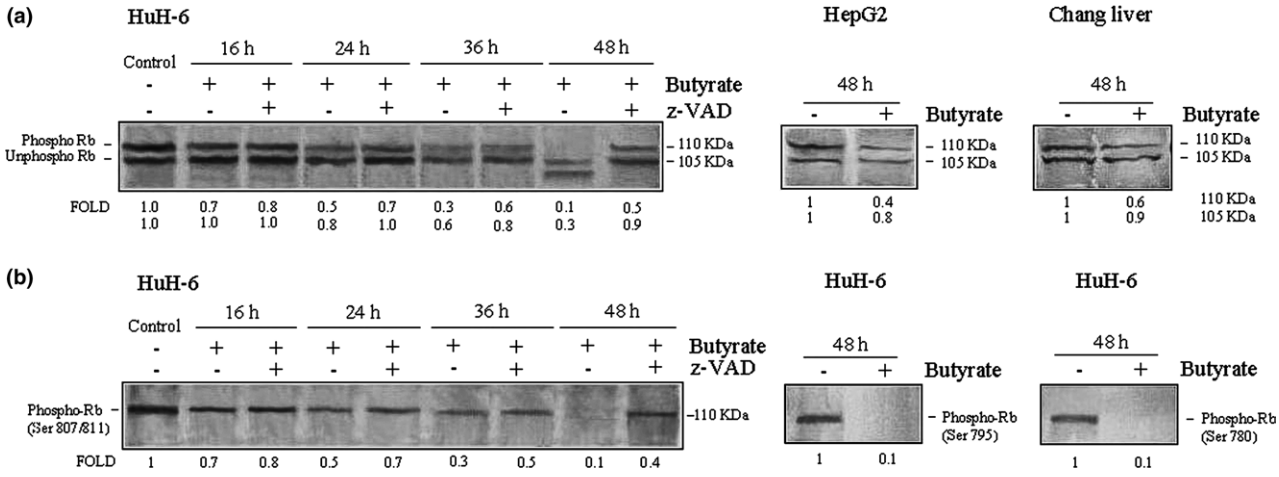

Fig. 5. Butyrate provoked dephosphorylation and cleavage of retinoblastoma protein. HuH-6, HepG2 or Chang liver cells exposed for various times to 2 mM sodium butyrate without or with 100 μM z-VAD. Cell lysates analysed by Western blotting in duplicate samples with the following antibodies: mouse monoclonal antibody, which recognises the A/B pocket of pRb (IF8) (a); phospho-pRb antibodies, which recognise pRb phosphorylated at ser 807 and 811 (b); ser 795 (c) or ser 780 (d). In (a) the unphosphorylated form of pRb appears as a fast migrating band, as compared to the slower migration of the phosphorylated form. Controls represent untreated samples at zero time of incubation. The intensity of bands was not modified by incubation for 48 h without butyrate. All experiments were performed three times with similar results.

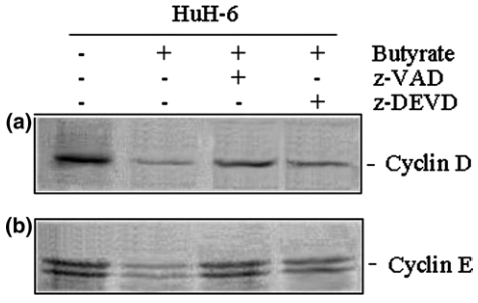

Fig. 6. Butyrate decreased the contents of cyclin D and cyclin E in HuH-6 cells. HuH-6 cells treated for 48 h with 2 mM sodium butyrate without or with 100 μM z-VAD-fmk or z-DEVD-fmk. Cell lysates analysed on duplicate samples by Western blotting for cyclin D and cyclin E. The results are representative of three independent experiments.

of control. The effects on Bcl-X isoforms were also dependent on the dose of butyrate employed (not shown).

The decrease in Bcl-X_L induced by butyrate was suppressed by the addition of z-VAD-fmk, a broad-spectrum caspase inhibitor, and markedly reduced by z-DEVD-fmk, a selective inhibitor of caspase 3 (Fig. 7(a)). These results suggested a possible involvement of caspase activity, and in particular of caspase 3, in the cleavage of Bcl-X_L. It is of interest to observe that neither of the two caspase inhibitors modified the increase induced by butyrate on the intensity of 21-kDa band. Therefore, it seems clear that the 21-kDa band was not a degradation product of Bcl-X_L. This consideration suggests that the 21-kDa band corresponds to Bcl-Xs.

Treatment of HepG2 cells with butyrate induced a very modest decrease in both Bcl-2 and Bcl-X_L together with the appearance of Bcl-Xs (not shown). Finally, in Chang liver cells, treatment with butyrate did not induce any significant modification in the content of the two anti-apoptotic factors Bcl-2 and Bcl-X_L (not shown).

It is known that butyrate can modulate the expression of genes correlated with apoptosis through histone hyperacetylation [2]. To determine whether the effect that butyrate exerted in HuH-6 cells on Bcl-X_L and Bcl-X_S proteins was transcriptionally regulated, we analysed Bcl-X mRNA species by semiquantitative RT-PCR. We used PCR primers that bind to sequences shared by Bcl-X_L and Bcl-Xs and flank the region that is deleted in Bcl-Xs. The two Bcl-X mRNA species can be distinguished as two bands of 780 and 490 bp, corresponding to Bcl-X_L and Bcl-Xs mRNA, respectively. Data reported in Fig. 7(b) show that treatment of HuH-6 cells with 2 mM butyrate for 48 h increased the production of mRNA transcripts for both Bcl-X_L and Bcl-Xs.

3.6. Butyrate induced loss of mitochondrial membrane potential

In many systems, apoptosis is associated with loss of mitochondrial inner membrane potential ($\Delta\psi_m$). In order to ascertain the role of mitochondria in butyrate-induced apoptosis, we tested the effects of butyrate on $\Delta\psi_m$ using DiOC6, a mitochondria-specific and voltage-dependent dye. Treatment of HuH-6 and HepG2 cells with butyrate resulted in an increase in the percentage of depolarised cells, which are characterised by low values of $\Delta\psi_m$. The effect, which was not observed in the first 16 h of treatment (not shown), appeared at 24 h of exposure and increased at 36 and 48 h (Fig. 8). The effect was more pronounced in HuH-6 cells than in HepG2 cells (not shown), while it was not observed in Chang

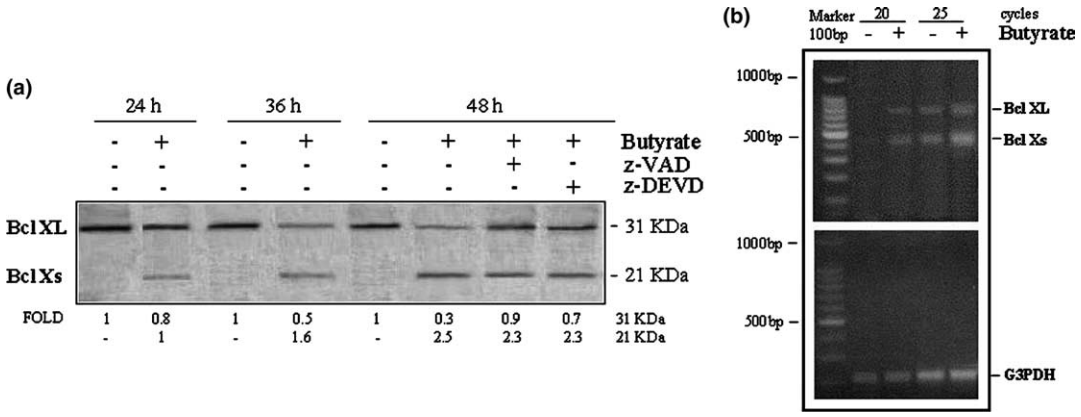

Fig. 7. The effect of butyrate on Bcl-X_L and Bcl-X_S proteins and the corresponding mRNAs in HuH-6 cells. (a) HuH-6 cells treated for various times with 2 mM sodium butyrate. Cell lysates analysed by Western blotting on duplicate samples for Bcl-X_L and Bcl-Xs using an antibody that recognises both isoforms. (b) Reverse transcriptase-polymerase chain reaction (PCR) used Bcl-X-specific primers and glyceraldehyde-3-phosphate dehydrogenase (G3PDH)-specific primers as control. The PCR products run on 2.5% agarose gels and visualised by ethidium bromide staining. A typical PCR result is shown. Bcl-Xs and Bcl-X_L mRNA increased after 48 h treatment with butyrate, whereas G3PDH mRNA was constant. The experiment was repeated three times and the intensity of bands was determined using a Kodak imaging system.

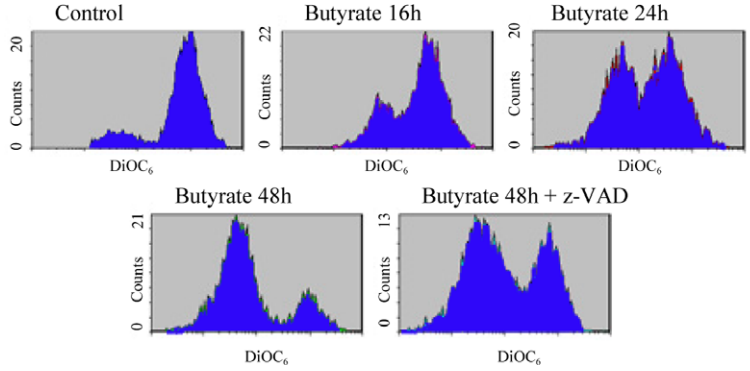

Fig. 8. Butyrate-induced mitochondrial transmembrane potential ($\Delta\psi_m$) transition in HuH-6 cells. HuH-6 cells treated with 2 mM sodium butyrate for various times without or with 100 μM z-VAD-fmk. $\Delta\psi_m$ quantified by flow cytometry with the lipophilic dye DiOC6. The results are representative of three independent experiments. The *x*-axis indicates the DiOC6 fluorescence intensity on a logarithmic scale; the *y*-axis indicates the number of events.

liver cells (not shown). The addition of 100 μM z-VAD-fmk had only a slight influence on the effect of butyrate in HuH-6 cells (Fig. 8). As a positive control for the reduction of $\Delta\psi_m$, HuH-6 cells were treated with the uncoupling agent CCCP (50 μM), which caused maximal $\Delta\psi_m$ disruption, corresponding to 100% of depolarised cells (not shown).

3.7. Butyrate-induced release of cytochrome c, activation of both caspase 9 and 3, and degradation of poly(ADP-ribose)-polymerase (PARP)

It has been demonstrated in many systems that a loss of $\Delta\psi_m$ can be responsible for the release of cytochrome *c* from the mitochondria into the cytosol with the consequent activation of the apoptosome complex and effector caspases [34]. Fig. 9(a) shows that treatment of HuH-6 cells with 2 mM butyrate caused a remarkable decrease in the amount of cytochrome *c* in the mitochondrial fraction and a concomitant increase in the cytosol.

To clarify whether caspase 9 was activated after exposure to butyrate, we examined the protein status by Western blot using an antibody that specifically recognises both the full-length p46 and the activated p35 forms. It was observed that treatment with 2 mM butyrate reduced the intensity of the band of pro-caspase 9, while a faster band of about 35 kDa appeared (Fig. 9(c)).

Moreover, treatment with butyrate reduced the intensity of the band of pro-caspase 3 at 32 kDa, while another band at 17 kDa appeared, corresponding to a component of caspase 3 (Fig. 9(d)). Both the effects on cytochrome *c* and on the caspases were not observed during the first 16 h of exposure to 2 mM butyrate; they appeared at 24 h and increased at 48 h. Treatment of

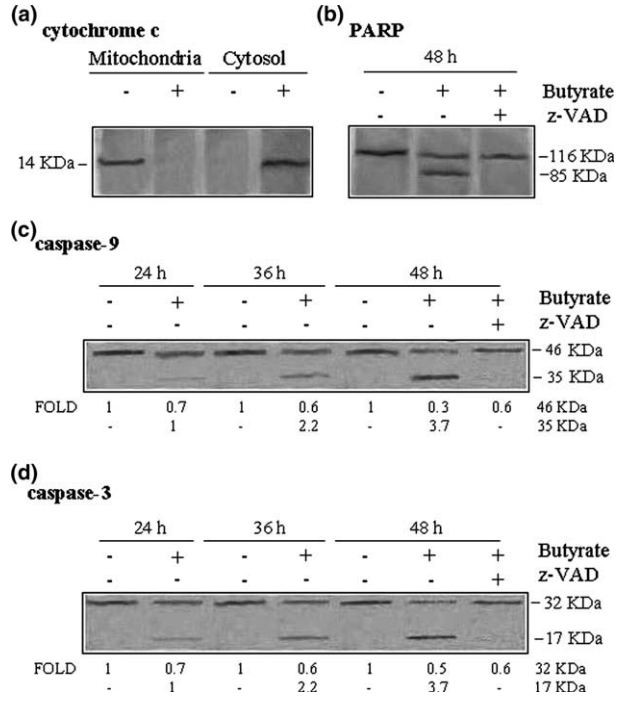

Fig. 9. Butyrate induced the release of cytochrome *c*, degradation of poly(ADP-ribose) polymerase (PARP) and the activation of caspase 9 and caspase 3 in HuH-6 cells. Cell lysates analysed by Western blotting in duplicate samples for cytochrome *c*, caspase 9, caspase-3 and PARP in HuH-6 cells treated with 2 mM butyrate for 48 h. The results are representative of three independent experiments.

HuH-6 cells with 2 mM butyrate also induced the degradation of PARP, a substrate of caspase 3. PARP degradation was revealed by the appearance of a fragment of 85 kDa (Fig. 9(b)).

4. Discussion

We demonstrated that butyrate induces apoptosis in both HuH-6 and HepG2 cells and that the effect appeared after a lag phase of approximately 16 h. Our aim was to ascertain the mechanism of the butyrate effect and to individuate the factors that protect the cells during the first phase of treatment.

We also showed that the sensitivity of HuH-6 cells to butyrate-induced apoptosis is higher than that exhibited by HepG2 cells, whereas in Chang liver cells butyrate did not produce a visible effect. We therefore intended to ascertain the reason for the different sensitivities exhibited by the three cell lines.

Among the factors that can protect cells against apoptosis, an important role may be exerted by β-catenin. It has been shown that deregulation of the Wnt–β-catenin pathway is a significant event in the development of hepatocellular carcinomas in man and mice and that somatic mutations of the β-catenin gene are frequent in human hepatocellular carcinomas [23,26]. Both HuH-6 and HepG2 cells contain altered forms of β-catenin [26]. Because degradation of these two forms is impaired they accumulate in the cytoplasm and in the nucleus, thereby stimulating genes involved in cell-cycle progression [19]. We demonstrate that treatment of hepatoma cells with butyrate induces a decrease in the content of β-catenin with a concomitant appearance of degradation products. This effect, which was marked in HuH-6 cells, was suppressed by z-VAD-fmk, suggesting that the degradation of β-catenin induced by butyrate is a consequence of the activation of caspases. It seems likely that caspase 3 played an important part in this event since the effects of butyrate were also consistently reduced by the specific inhibitor z-DEVD-fmk.

In order to address whether the accumulation of β-catenin in HuH-6 cells could favour cell survival by exerting an anti-apoptotic effect, we pretreated HuH-6 cells with a β-catenin antisense ODN. Our results provide evidence that this pretreatment reduced the amount of β-catenin, anticipated the onset of butyrate-induced apoptosis at 8 h and potentiated the effect of the drug. These findings strongly suggest that the marked decrease in β-catenin observed during the second day of treatment with butyrate can increase the sensitivity of HuH-6 cells to this compound. However, the mechanism by which β-catenin affects apoptosis is unknown. At the moment our results do not allow us to establish whether the protective action against apoptosis is a peculiar character of the altered form of β-catenin that accumulates in HuH-6 cells or a general character also exhibited by the wild-type form of the protein. We have scheduled new experiments in our laboratory in order to clarify this aspect.

In this paper we focus on the effects of butyrate on the content of pRb and on its phosphorylation state. It is well known that pRb exerts an anti-proliferative effect [28]. In the hypophosphorylated form it assembles and inhibits the activity of E2F [29], a transcription factor with an important role in cell-cycle progression. pRb becomes hyperphosphorylated in the late G1 phase [29] by CDK–cyclin complexes and remains in this state throughout S, G2 and M. Phosphorylation of pRb causes the release of E2F [29], which through interaction with DP produces a heterodimeric complex, thereby stimulating the expression of S-phase genes [29]. Moreover, pRb also plays a part in the terminal differentiation of many cells, acting in its unphosphorylated form as a transcriptional coactivator or modulator by binding to and potentiating the activity of a number of transcription factors with a specific role in differentiation [30]. In addition, pRb has been shown to exert a protective action against apoptosis [31], which can be explained by the fact that it binds several proteins with pro-apoptotic functions, such as c-Abl [35], JNK [36] and in particular E2F-1 [37]. This last factor plays a part not only in the expression of S-phase genes, but also in

that of genes that encode components of the cell-death machinery, including caspase 3 [38] and APAF-1 [39], a key part of the apoptosome.

Chau and Wang [31] proposed a model in which pRb produces complexes with E2F that are assembled either at the promoters of S-phase genes or at the promoters of apoptotic genes. They suggest that phosphorylation of pRb only disrupts the complexes at the promoters of S-phase genes, while pRb degradation would be required to disrupt the complexes at the promoters of apoptotic genes. We show that treatment with butyrate lowers both phosphorylated and unphosphorylated forms of pRb. In addition, our results suggest that dephosphorylation of pRb precedes degradation of the protein. The finding that z-VAD-fmk, a general inhibitor of caspases, completely suppressed the effect of butyrate on unphospho-pRb strongly suggests that the decrease in the amount of this form is determined by the cleavage of the protein by caspases. According to Chau and Wang [31], we advance the hypothesis that the cleavage of pRb may cause the activation of apoptotic genes and, consequently, the acceleration of apoptosis observed during the second day of treatment.

Our results suggest that the dephosphorylation of pRb may partly be caused by the reduction in the amounts of cyclins D and E, two factors necessary for the activity of CDK4 and CDK2, respectively, that are involved in the phosphorylation of pRb during the cell cycle 29]. Also, the fall in cyclin contents seemed to be a consequence of the activation of caspases, since the addition of z-VAD-fmk or z-DEVD-fmk prevented the effect of butyrate on cyclins D and E. However, because z-VAD-fmk only partly reduced the effect of butyrate on the phosphorylated form of pRb, we conclude that other mechanisms different from the activation of caspases may exert a role in the dephosphorylation of pRb.

It is well known that the proteins of Bcl-2 family exert a fundamental role in the fate of cells, since some members of this family favour cell survival while others are involved in the induction of apoptosis [40]. In this regard it is interesting that HuH-6 cells are lacking in the anti-apoptotic factor Bcl-2, while HepG2 cells contain a low amount of this factor. Survival of hepatoma cells is most probably assured by the presence in both HuH-6 cells and HepG2 cells of large amounts of Bcl-X_L, a powerful anti-apoptotic factor, while the pro-apoptotic factor Bcl-Xs, the other isoform generated from the *Bcl-X* gene, is undetectable in both cell lines. Our results demonstrate that treatment of HuH-6 cells with butyrate induces remarkable modifications in the amounts of Bcl-X isoforms. Bcl-X_L was markedly lowered, an effect that was clearly observed during the second day of treatment. This event seemed to be a consequence of activation of caspases and in particular of caspase 3, because the addition of caspase inhibitors prevented the effect of butyrate on Bcl-X_L. Differently, in treated cells we observed during the second day of treatment a remarkable increase in the intensity of a 21-kDa band, which was recognised as Bcl-X_S, an effective apoptotic factor. This effect most probably depended on the increased expression of the *Bcl-X* gene, since analysis of Bcl-X mRNA species by RT-PCR showed that butyrate increased Bcl-Xs transcripts. The contemporaneous increase in the Bcl-X_L transcript can be considered as a compensatory response to the degradative effect induced by butyrate.

We show that butyrate induced the loss of $\Delta\psi_m$ and the release of cytochrome *c* from mitochondria to the cytoplasm, indicating the involvement of mitochondria in apoptosis. Moreover, the increase of cytochrome *c* in the cytoplasm was most probably the cause of the activation of caspase 3, which was associated with the degradation of PARP, a specific substrate of caspase 3. It seems that the activation of caspase occurred later than transmembrane potential disruption because the addition of the pan-caspase inhibitor z-VAD-fmk had only a modest effect on the loss of $\Delta\psi_m$. We also suggest that the involvement of mitochondria as well as the release of cytochrome *c* and the activation of caspase 3 were correlated with the modifications in the amount of Bcl-X isoforms induced by butyrate. This conclusion is in line with other studies showing that Bcl-X_L plays a crucial part in maintaining mitochondrial membrane potential [41] and in inhibiting the release of cytochrome *c* [41], while Bcl-Xs has been shown to be involved in the activation of caspase 3 [42].

Taken together our results demonstrate that β-catenin, pRb and Bcl-X_L are present at high concentrations in HuH-6 cells and suggest a protective role for these factors in preventing apoptosis. With butyrate, HuH-6 cells are stimulated to produce Bcl-Xs, a pro-apoptotic factor capable of inducing the effector caspases that trigger apoptosis. Activation of caspases seems have a fundamental role in butyrate-induced apoptosis, thereby favouring the degradation of β-catenin, cyclins, pRb and Bcl-X_L. This paper proposes a role for β-catenin in cell survival and demonstrates that reducing the amount of this protein in cells where it has accumulated facilitates the induction of apoptosis by butyrate. Moreover, it is noteworthy that the cleavage of Bcl-X_L by caspases could originate an amplification loop in mitochondrial events. These effects are most probably responsible for accelerating the apoptotic action of butyrate, which occurred on the second day of treatment.

It is of interest that the effects induced by butyrate in HepG2 cells on the activation of caspases and on the contents of Bcl-Xs, Bcl-X_L, pRb and β-catenin were smaller than in HuH-6 cells. This finding was consistent with the lower sensitivity to butyrate-induced apoptosis exhibited by HepG2 cells in comparison to HuH6 cells.

In Chang liver cells, Bcl-2 exerts an important role in protection against apoptosis and is the major protective agent in these cells. The observation that in Chang liver

cells butyrate was unable to enhance the content of Bcl-Xs or to reduce the contents of Bcl-2 and Bcl-X_L is in accord with the inability of butyrate in the induction of apoptosis in these cells.

Sodium butyrate and its analogues are currently under clinical investigation for potential anti-cancer activity. The results shown here suggest that these compounds may have importance in novel therapeutic strategies for hepatoma.

Acknowledgements

This study was partially supported by the Italian Ministry of University and Scientific Technological Research, MURST-PRIN (2000). The work of A. D'Anneo was supported by a fellowship grant from Associazione Italiana per la Ricerca sul Cancro (AIRC).

References

1. Harrison LE, Wang QM, Studzinski GP. Butyrate-induced G2 block in CaCo-2 colon cancer cells is associated with decreased $p34^{cdc2}$ activity. *Proc Soc Exp Biol Med* 1999, **222**, 150–156.
2. Koyama Y, Adachi M, Sekiya M, Takekawa M, Imai K. Histone deacetylase inhibitors suppress IL-2-mediated gene expression prior to induction of apoptosis. *Blood* 2000, **96**, 1490–1495.
3. Pellizzaro C, Coradini D, Daniotti A, Abolafio G, Dandone MG. Modulation of cell cycle-related protein expression by sodium butyrate in human non-small cell lung cancer cell lines. *Int J Cancer* 2001, **91**, 654–657.
4. Finzer P, Kuntzen C, Soto U, zur Hausen H, Rosl F. Inhibitors of histone deacetylase arrest cell cycle and induce apoptosis in cervical carcinoma cells circumventing human papillomavirus oncogene expression. *Oncogene* 2001, **20**, 4768–4776.
5. Couchie D, Holic N, Chobert MN, Corlu A, Laperche Y. In vitro differentiation of WB-F344 rat liver epithelial cells into the biliary lineage. *Differentiation* 2002, **69**, 209–215.
6. Khan KN, Tsutsumi T, Nakata K, Kato Y. Sodium butyrate induces alkaline phosphatase gene expression in human hepatoma cells. *J Gastroenterol Hepatol* 1999, **14**, 156–162.
7. Tabuchi Y, Arai Y, Kondo T, Takeguchi N, Asano S. Identification of genes responsive to sodium butyrate in colonic epithelial cells. *Biochem Biophys Res Commun* 2002, **293**, 1287–1294.
8. Soldatenkov VA, Prasad S, Voloshin Y, Dritschilo A. Sodium butyrate induces apoptosis and accumulation of ubiquitinated proteins in human breast carcinoma cells. *Cell Death Diff* 1998, **5**, 307–312.
9. Hernandez A, Thomas R, Smith F, *et al*. Butyrate sensitizes human colon cancer cells to TRAIL-mediated apoptosis. *Surgery* 2001, **130**, 265–272.
10. Kamitani H, Taniura S, Watanabe K, Sakamoto M, Watanabe T, Eling T. Histone acetylation may suppress human glioma cell proliferation when p21 WAF/Cip1 and gelsolin are induced. *Neuro-oncology* 2002, **4**, 95–101.
11. Mohiuddin I, Cao X, Fang B, Nishizaki M, Smythe WR. Significant augmentation of pro-apoptotic gene therapy by pharmacologic Bcl-X_L down-regulation in mesothelioma. *Cancer Gene Ther* 2001, **8**, 547–554.
12. Chopin V, Toillon RA, Jouy N, Le Bourhis X. Sodium butyrate induces P53-independent, Fas-mediated apoptosis in MCF-7 human breast cancer cells. *Br J Pharmacol* 2002, **135**, 79–86.
13. Cao X, Mohuiddin I, Ece F, McConkey DJ, Smythe WR. Histone deacetylase inhibitor downregulation of Bcl-X_L gene expression leads to apoptotic cell death in mesothelioma. *Am J Respir Cell Mol Biol* 2001, **25**, 562–568.
14. Saito H, Ebinuma H, Takahashi M, Kaneko F, Wakabayashi K, Nakamura M, *et al*. Loss of butyrate-induced apoptosis in human hepatoma cell lines HCC-M and HCC-T having substantial Bcl-2 expression. *Hepatology* 1998, **27**, 1233–1240.
15. Yamamoto H, Fujimoto J, Okamoto E, Furuyama J, Tamaoki T, Hashimoto-Tamaoki T. Suppression of growth of hepatocellular carcinoma by sodium butyrate in vitro and in vivo. *Int J Cancer* 1998, **76**, 897–902.
16. Wang XM, Li J, Evers BM. Inhibition of proliferation, invasion and adhesion of liver cancer cells by 5-azacytidine and butyrate. *Anticancer Res* 1999, **19**, 2901–2906.
17. Giuliano M, Lauricella M, Calvaruso G, Emanuele S, Vento R, Tesoriere G. The apoptotic effects and synergistic interaction of sodium butyrate and MG132 in human retinoblastoma Y79 cells. *Cancer Res* 1999, **59**, 5586–5595.
18. Lauricella M, Calvaruso G, Giuliano M, Emanuele S, Vento R, Tesoriere G. Synergistic cytotoxic interactions between sodium butyrate, MG132 and camptothecin in human retinoblastoma Y79 cells. *Tumor Biol* 2000, **21**, 337–348.
19. Liu CJ, Chen PJ, Shau WY, Kao JH, Lai MY, Chen DS. Clinical aspects and outcomes of volunteer blood donors testing positive for hepatitis-C virus infection in Taiwan: a prospective study. *Liver* 2003, **23**, 148–155.
20. Ming L, Thorgeirsson SS, Gail MH, *et al*. Dominant role of hepatitis B virus and cofactor role of aflatoxin in hepatocarcinogenesis in Qidong, China. *Hepatology* 2002, **36**, 1214–1220.
21. Park KA, Kweon S, Choi H. Anticarcinogenic effect and modification of cytochrome P450 2E1 by dietary garlic powder in diethylnitrosamine-initiated rat hepatocarcinogenesis. *J Biochem Mol Biol* 2002, **35**, 615–622.
22. Bright-Thomas RM, Hargest R. APC, beta-catenin and hTCF-4; an unholy trinity in the genesis of colorectal cancer. *Eur J Surg Oncol* 2003, **29**, 107–117.
23. Buendia MA. Genetic alterations in hepatoblastoma and hepatocellular carcinoma: common and distinctive aspects. *MED Pediatr Oncol* 2002, **39**, 530–535.
24. Lauricella M, Calvaruso G, Giuliano M, Emanuele S, Vento R, Tesoriere G. pRb suppresses camptothecin-induced apoptosis in human osteosarcoma Saos-2 cells by inhibiting c-Jun N-terminal kinase. *FEBS Lett* 2001, **499**, 191–197.
25. Chomczynski P, Sacchi N. Single-step method of RNA isolation by acid guanidinium thiocyanate–phenol–chloroform extraction. *Anal Biochem* 1987, **162**, 156–159.
26. De la Coste A, Romagnolo B, Billuart P, *et al*. Somatic mutations of beta-catenin gene are frequent in mouse and human hepatocellular carcinomas. *Proc Natl Acad Sci USA* 1998, **95**, 8847–8851.
27. Fukuda K. Apoptosis-associated cleavage of beta-catenin in human colon cancer and rat hepatoma cells. *Int J Biochem Cell Biol* 1999, **3**, 519–529.
28. Yamasaki L. Role of the RB tumor suppressor in cancer. *Cancer Treat Res* 2003, **115**, 209–239.
29. Stevens C, La Thangue NB. E2F and cell cycle control: a double-edged sword. *Arch Biochem Biophys* 2003, **412**, 157–169.
30. Yee AS, Shih HH, Tevosian SG. New perspectives on retinoblastoma family functions in differentiation. *Front Biosci* 1998, **3**, 532–547.
31. Chau BN, Wang JY. Coordinated regulation of life and death by RB. *Nat Rev Cancer* 2003, **3**, 130–138.

32. An B, Johonson DE, Jin JR, Antoku K, Dou QP. Bcl-2- and CrmA-inhibitable dephosphorylation and cleavage of retinoblastoma protein during etoposide-induced apoptosis. *Int J Mol Med* 1998, **1**, 131–136.
33. Chen WD, Otterson GA, Lipkowitz S, Khleif SN, Coxon AB, Kaye FJ. Apoptosis is associated with cleavage of a 5 kDa fragment from RB which mimics dephosphorylation and modulates E2F binding. *Oncogene* 1997, **14**, 1243–1248.
34. Nencioni A, Lauber K, Grunebach F, *et al*. Cyclopentenone prostaglandins induce lymphocyte apoptosis by activating the mitochondrial apoptosis pathway independent of external death receptor signaling. *J Immunol* 2003, **171**, 5148–5156.
35. Welch PJ, Wang JY. C-terminal protein-binding domain in the retinoblastoma protein regulates nuclear c-Abl tyrosine kinase in the cell cycle. *Cell* 1993, **75**, 779–790.
36. Shim J, Park HS, Kim MJ, *et al*. Rb protein down-regulates the stress-activated signals through inhibiting c-Jun N-terminal kinase/stress-activated protein kinase. *J Biol Chem* 2000, **275**, 14107–14111.
37. Morris EJ, Dyson NJ. Retinoblastoma protein patterns. *Adv Cancer Res* 2001, **82**, 1–54.
38. Muller H, Bracken AP, Vernell R, *et al*. E2Fs regulate the expression of genes involved in differentiation, development, proliferation and apoptosis. *Genes Dev* 2001, **15**, 267–285.
39. Moroni MC, Hickman ES, Denchi EL, *et al*. Apaf-1 is a transcriptional target for E2F and p53. *Nat Cell Biol* 2001, **3**, 552–558.
40. Tsujimoto Y. Cell death regulation by the Bcl-2 protein family in the mitochondria. *J Cell Physiol* 2003, **195**, 158–167.
41. Sun XM, Bratton SB, Butterworth M, MacFarlane M, Cohen GM. Bcl-2 and Bcl-XL inhibit CD95-mediated apoptosis by preventing mitochondrial release of Smac/Diablo and subsequent inactivation of X-linked inhibitor of apoptosis protein. *J Biol Chem* 2002, **277**, 11345–11351.
42. Rong P, Bennie AM, Epa WR, Barrett GL. Nerve growth factor determines survival and death of PC12 cells by regulation of the Bcl-X, bax and caspase-3 genes. *J Neurochem* 1999, **72**, 2294–2300.